Prediction of total corneal power from measured anterior corneal power on the IOLMaster 700 using a feedforward shallow neural network

Achim Langenbucher,[1] Alan Cayless,[2] Nóra Szentmáry,[3,4] Johannes Weisensee,[1] Jascha Wendelstein[5] and Peter Hoffmann[6]

[1]Department of Experimental Ophthalmology, Saarland University, Homburg/Saar, Germany
[2]School of Physical Sciences, The Open University, Milton Keynes, UK
[3]Dr. Rolf M. Schwiete Center for Limbal Stem Cell and Aniridia Research, Saarland University, Homburg/Saar, Germany
[4]Department of Ophthalmology, Semmelweis-University, Budapest, Hungary
[5]Department of Ophthalmology, Johannes Kepler University Linz, Linz, Austria
[6]Augen- und Laserklinik Castrop-Rauxel, Castrop-Rauxel, Germany

ABSTRACT.

Background: The corneal back surface is known to add some astigmatism against-the-rule, which has to be considered in cataract surgery with toric lens implantation. The purpose of this study was to set up a deep learning algorithm which predicts the total corneal power from keratometry and biometric measures.

Methods: Based on a large data set of measurements with the IOLMaster 700 from two clinical centres, data from $N = 21\,108$ eyes were included, each record containing valid data for keratometry K, total keratometry TK, axial length AL, central corneal thickness CCT, anterior chamber depth ACD, lens thickness LT and horizontal corneal diameter W2W from an individual eye. After a vector decomposition of K and TK into equivalent power (.EQ) and projections of astigmatism to the $0°/90°$ (.AST$_{0°}$) and $45°/135°$ (.AST$_{45°}$) axis, a multi-output feedforward shallow neural network was derived to predict TK from K, AL, CCT, ACD, LT, W2W and patient age.

Results: After some trial and error, the neural network having a Levenberg–Marquardt training function and three hidden layers (10/8/5 neurons) performed best and showed a fast convergence. The data set was split into training data (70%), validation data (15%) and test data (15%). The prediction error (predicted corneal power CP$_{pred}$ minus TK) of the network trained with the training and cross-validated with test data showed systematically narrower distributions for CPEQ-TKEQ, CPAST$_{0°}$-TKAST$_{0°}$ and CPAST$_{45°}$-TKAST$_{45°}$ compared with KEQ-TKEQ, KAST$_{0°}$-TKAST$_{0°}$ and KAST$_{45°}$-TKAST$_{45°}$. There was no systematic offset in the components between CP$_{pred}$ and TK.

Conclusion: Unlike any fixed correction term, which can compensate only for a static intercept of the astigmatic components TKEQ, TKAST$_{0°}$ and TKAST$_{45°}$ compared with KEQ, KAST$_{0°}$ and KAST$_{45°}$, our trained neural network was able to reduce the variance in the prediction error significantly. This neural network could be used to account for the corneal back surface astigmatism for biometers where the corneal back surface measurement or total keratometry is not available.

Key words: biometry – corneal back surface – deep learning – feedforward multi-output network – neural network – posterior corneal astigmatism

Background

In 1999 with the IOLMaster, the first optical biometer was launched to the market (Haigis et al. 2000; Chen et al. 2011). In contrast to ultrasound biometers which are restricted to a measurement of distances in the eye such as axial length (AL), central corneal thickness (CCT), anterior chamber depth (ACD) and lens thickness (LT), the IOLMaster was able to assess AL using partial coherence interferometry and corneal curvature of the front surface with an integrated keratometer. The phakic anterior chamber depth could be derived using an integrated Scheimpflug camera, and

the horizontal corneal diameter (W2W) was assessed by means of a simple photo with green light (red-free) (Chen et al. 2011). Overall, the measurements from a single instrument were sufficient to determine the refractive power of intraocular lenses as performed directly with the software tools of the IOL-Master. Compared with ultrasound techniques, where the measurement of distances depends on the speed of sound which varies significantly (e.g. for different degrees of cataract densities or silicone oil as replacement for native vitreous humour), optical biometry shows much less variation since the refractive index of the media does not vary that much from the cataract or vitreous stage.

With the next generations of optical biometers, mostly based on low coherence reflectometry or optical coherence tomography (OCT), it was possible to derive additional measures such as the CCT and LT, and the ACD (or aqueous depth as the distance from corneal endothelium to the lens front vertex) is also mostly measured with the same technique, which, together with new lens calculation formulae and better formula constant optimization, significantly improved the predictability of the refractive outcome after cataract surgery (Chen et al. 2011; Fisus, Hirnschall & Findl 2021; Fisus, Hirnschall et al. 2021).

In the last couple of years, the trends of optical biometry have been towards measuring total keratometry considering corneal front and back surface measurement. The first instrument capable of measuring both corneal surfaces was launched in 2013 with the IOLMaster 700 (Fisus, Hirnschall & Findl 2021; Fisus, Hirnschall et al. 2021; Langenbucher et al. 2021). In addition to keratometric measurement of the corneal front surface curvature at 18 points, a software option provides data of the corneal thickness profile and the corneal back surface curvature based on a 3-dimensional OCT scan. In addition to the keratometric power, the power of the corneal back surface (as well as central corneal thickness) is extracted from the data of the 3D OCT scan. From both corneal surfaces and central corneal thickness data, the total corneal power is derived using the Gullstrand formula for toric surfaces and could be used for lens power calculations.

Artificial intelligence and specifically machine learning algorithms have developed significantly in recent years. Today, they are used in many disciplines in medicine (e.g. for diagnosis or classification of diseases or clustering purposes) and in other fields. In most of the tasks supervised, learning strategies are used, involving a large data set with labels (either categorical data from a classification or metric data as target value). The classification or regression neural network is trained with this data set to reproduce this classification or to predict the metric value based on the input data. To evaluate the performance of such a neural network, the data set has to be split into training data and validation or test data. The training data are used to train the network, and the validation and test data are used to cross-validate the prediction and to avoid overfitting.

The purpose of this study was to show, using a large data set from the IOLMaster 700, whether a shallow feedforward neural network architecture could predict the vector components of total corneal power from the respective vector components of keratometric power and AL, CCT, ACD, LT, W2W and patient's age, and whether such a prediction could be used, for example, with optical biometers which do not provide corneal back surface curvature data.

Methods

Data set for the neural network

In total, a data set with 48 455 measurements from the IOLMaster 700 (Zeiss, Jena, Germany) from 2 clinical centres (Augenklinik Castrop, Germany and Kepler University, Linz, Austria) was considered for this retrospective study. All biometry measurements were performed prior to cataract surgery. The data were transferred to a.csv data table using the data export and backup module of the software. In a next step, the tables from both clinical centres were merged. Duplicate measurements of eyes were discarded by selecting the last examination before cataract surgery. Missing data or data with a 'Failed' or 'Warning' in the quality check for keratometry, AL, CCT, ACD, LT, W2W, date of birth or examination date provided by the IOLMaster 700 software were excluded, and after checking for 'Successful' measurement for corneal back surface power and total corneal power, a data set containing records of measurements from $N = 21\,108$ eyes was used for training, validation and test of our neural network. The data were transferred to Matlab (Matlab 2019b; MathWorks, Natick, MA, USA) for further processing.

Preprocessing of the data

Custom software was written in Matlab to derive the patient age from the examination date and date of birth. From the keratometric data (K) of the corneal front surface curvature measurement (flat radius R1, axis of the flat radius A1, steep radius R2 and axis of the steep radius A2), the refractive power in both cardinal meridians was derived using a keratometer index of $n_K = 1.332$, and the 3 vector components KEQ, $KAST_{0°}$ and $KAST_{45°}$ were calculated: the equivalent power KEQ was extracted from the arithmetic mean of $K1 = (1.332-1.0)/R1$ and $K2 = (1.332-1.0)/R2$. The keratometric astigmatism $KAST = (K2-K1)$ was projected to the 0°/90° axis with $KAST_{0°} = KAST·\cos(2·A1)$ and to the 45°/135° axis with $KAST_{45°} = KAST·\sin(2·A1)$ (Alpins et al. 1994). For the total keratometry (TK) (flat radius TR1, axis of the flat radius TA1, steep radius TR2 and axis of the steep radius TA2), the refractive power in both cardinal meridians was derived using a keratometer index of $n_K = 1.332$, and the three vector components TKEQ, $TKAST_{0°}$ and $TKAST_{45°}$ were calculated: the equivalent power TKEQ was extracted from the arithmetic mean of $TK1 = (1.332-1.0)/TR1$ and $TK2 = (1.332-1.0)/TR2$. The total corneal astigmatism $TKAST = (TK2-TK1)$ was projected to the 0°/90° axis with $TKAST_{0°} = -TKAST·\cos(2·TA1)$ and to the 45°/135° axis with $TKAST_{45°} = TKAST·\sin(2·TA1)$ (Alpins et al. 1994). As target or output variables, we considered the predicted total corneal power CP_{pred} in terms of three vector components: equivalent power (CPEQ), astigmatism projected to 0°/90° axis ($CPAST_{0°}$) and 45°/135° axis ($CPAST_{45°}$) (Alpins et al. 1994).

Set up of the neural network

A feedforward shallow multilayer multi-output neural network was set up for predicting the total corneal power

CP_{pred} from the keratometric power K and distances as well as patient age (Zell 1994; Schmidhuber 2015). Feedforward (in contrast to recurrent) neural networks are implementations of an artificial multilayer neural network where the nodes of a hidden layer only have connections to the subsequent hidden layer (i.e. feedforward) and do not have any feedback connections to the previous layer. In this context, 'shallow' refers to a neural network structure with only few hidden layers, and 'multi-output' to the fact that more than one output value is predicted by the neural network (in our case: three vector components of CP_{pred}), in contrast to a classical neural network with one output value.

From keratometry K, we used the vector components KEQ, $KAST_{0°}$ and $KAST_{45°}$. For the distances, we included AL, CCT, ACD, LT and W2W. Each patient's age was derived from the examination date and the date of birth. In addition, we built up a smart version of our neural network, including only AL, ACD, and W2W in addition to keratometry, as these data were already available in the first generation of optical biometers. We designed our neural network with multiple outputs to predict CP_{pred} (CPEQ, $CPAST_{0°}$ and $CPAST_{45°}$) in one step. Several training algorithms and several network architectures with 2, 3 and 4 hidden layers were tested, for example the simple form of gradient descent with or without momentum, scaled conjugate gradient, quasi-Newton, Bayesian regularization or Levenberg–Marquardt. Finally, we proved that with our data set the Levenberg–Marquardt training algorithm with three hidden layers and 10/8/5 neurons in layer 1/2/3 performed best for predicting the total corneal power CP_{pred}. Backpropagation techniques were applied for computing the gradients and Jacobian matrices as well as for defining the weighting functions. The performance of the network was evaluated with the unweighted sum of mean squared prediction error

The data set with $N = 21\,108$ measurements was split using a random selection into a training set (70%, $N = 14{,}776$), a validation set ($N = 3166$) and a test set ($N = 3166$). The neural network was trained with the training data set and later validated with the validation data set. Final proof was performed using the $N = 3166$ test data set.

Validation process

Validation of our feedforward neural network was performed with quality metrics in terms of mean (MEAN) and median (MED) prediction error, minimum (MIN) and maximum (MAX) prediction error, together with the mean absolute (MAE) of all 3 target variables CPEQ, $CPAST_{0°}$ and $CPAST_{45°}$. The 3 vector components of CP_{pred} were compared with keratometry K (KEQ, $KAST_{0°}$, $KAST_{45°}$) and also to total corneal power provided by the IOLMaster 700 (TKEQ, $TKAST_{0°}$ and $TKAST_{45°}$). The quality metrics were calculated for the test data and for the entire data set.

Results

The descriptive statistics of the relevant variables in our data set with $N = 21\,108$ measurements is shown in Table 1 in terms of mean, standard deviation, median, minimum and maximum. After training the neural network, the performance plot provided in Figure 1 shows the mean squared error for the training set ($N = 14\,776$), the validation set ($N = 3166$) and for the test set ($N = 3166$) as a function of the number of iteration or training cycles (epochs). The feedforward network shows a fast convergence, reaching the final performance after 9 epochs of iteration as indicated by the cyan line. The respective mean squared errors for the training set, the validation set and the test set are shown in the legend of the graph.

Table 2 lists the descriptive performance data of the trained network applied to the test data set ($N = 3166$)

for cross-validation. In this table, the mean, standard deviation, median, minimum and maximum of the prediction error (CP_{pred}-TK) and for comparison the difference K-TK are shown for the equivalent power (CPEQ-TKEQ and KEQ-TKEQ) as well as for the projections of the astigmatism to the 0°/180° axis ($CPAST_{0°}$-$TKAST_{0°}$ and $KAST_{0°}$-$TKAST_{0°}$) and the 45°/135° axis ($CPAST_{45°}$-$TKAST_{45°}$ and $KAST_{45°}$-$TKAST_{45°}$), respectively.

Figure 2A–C shows, using combined scatterhist plots, the prediction error CP_{pred} minus total corneal power TK provided by the IOLMaster 700 together with the distribution of the respective keratometer measures K minus TK for the three vector components. The scatterhist plots combine a scatterplot and a graph showing the distribution function (fit with a kernel distribution). In Figure 2A, the prediction error for the equivalent power CPEQ-TKEQ is plotted alongside the difference between keratometric equivalent power K and total corneal power TK. The distribution of CPEQ-TKEQ is much narrower compared with the distribution of K-TKEQ, meaning that the neural network shows a good performance in predicting the total corneal power equivalent from keratometry and biometric measures. In Figure 2B, the prediction error for the astigmatism projected to the 0°/180° axis ($CPAST_{0°}$-$TKAST_{0°}$) is plotted together with the difference between keratometric (K) and total corneal power (TK) astigmatism projected to the 0°/180° axis ($KAST_{0°}$-$TKAST_{0°}$). The distribution of ($KAST_{0°}$-$TKAST_{0°}$) is systematically shifted to negative values, meaning that, in general, the corneal back surface adds some astigmatism with a magnitude of around 0.2 dpt against-the-rule (with an orientation of around 90°). Again, the distribution of $CPAST_{0°}$-$TKAST_{0°}$ is narrower (see also Table 2) compared with the distribution of $KAST_{0°}$-$TKAST_{0°}$, meaning that the neural network shows a good performance in predicting the total corneal power

$$\text{performance} = \frac{\sum_{N}(CPEQ - TKEQ)^2 + \sum_{N}(CPAST_{0°} - TKAST_{0°})^2 + \sum_{N}(CPAST_{45°} - TKAST_{45°})^2}{3 \cdot N}.$$

Table 1. Descriptive statistics of the data used for the processing of input and output data. R1 and R2 refer to the corneal front surface radius at the flat and steep meridian, TR1 and TR2 to the respective data of total keratometry (radius in the flat (TR1) and steep (TR2) meridian), and AL / CCT / ACD / LT / W2W to the axial length / central corneal thickness / phakic anterior chamber depth / crystalline lens thickness / horizontal corneal diameter. The respective axes of keratometry and total corneal power are not listed in this table

N = 21 108	R1 in mm	R2 in mm	TR1 in mm	TR2 in mm	Age in years	AL in mm	CCT in mm	ACD in mm	LT in mm	W2W in mm
Mean	7.7942	7.6284	7.7969	7.6270	68.89	23.6774	0.5520	3.1335	4.6127	11.9787
SD	0.2842	0.2841	0.2869	0.2832	12.21	1.3972	0.0372	0.4186	0.4899	0.4105
Median	7.7846	7.7688	7.7873	7.6265	72.00	23.4908	0.5514	3.1282	4.6405	11.9771
Minimum	6.0368	5.2423	6.0754	5.2717	52.00	14.5852	0.3882	1.1876	3.0048	8.9941
Maximum	9.7572	9.2428	9.8842	9.4453	100.00	37.5372	0.9268	5.3148	6.6412	14.8809

astigmatic component with/against-the-rule from keratometry and biometric measures. In Figure 2C, the prediction error for the astigmatism projected to the oblique 45°/135° axis (CPAST$_{45°}$-TKAST$_{45°}$) is plotted alongside with the difference between keratometric (K) and total corneal power (TK) astigmatism projected to the 45°/135° axis (KAST$_{45°}$-TKAST$_{45°}$). For the oblique axis, the distribution of (KAST$_{45°}$-TKAST$_{45°}$) is not systematically shifted. However, the distribution of CPAST$_{45°}$-TKAST$_{45°}$ is again narrower (see also Table 2) compared with the distribution of KAST$_{45°}$-TKAST$_{45°}$, meaning that the neural network shows a good performance in predicting the total corneal power astigmatic component in the oblique axis from keratometry and biometric measures

In Table 3, we list the prediction error of the smart version of our feedforward shallow neural network, which considers only AL, ACD and W2W as input parameters in addition to keratometry based on corneal front surface curvature as these measures have been available since 1999 even with the initial version of the IOL-Master as well as by all other optical biometers on the market. Even though the distributions of the 3 components of the prediction error are narrower compared with the distributions of the difference of K-TK, the overall performance is systematically worse compared with the full version of the neural network as shown before with the respective performance metrics
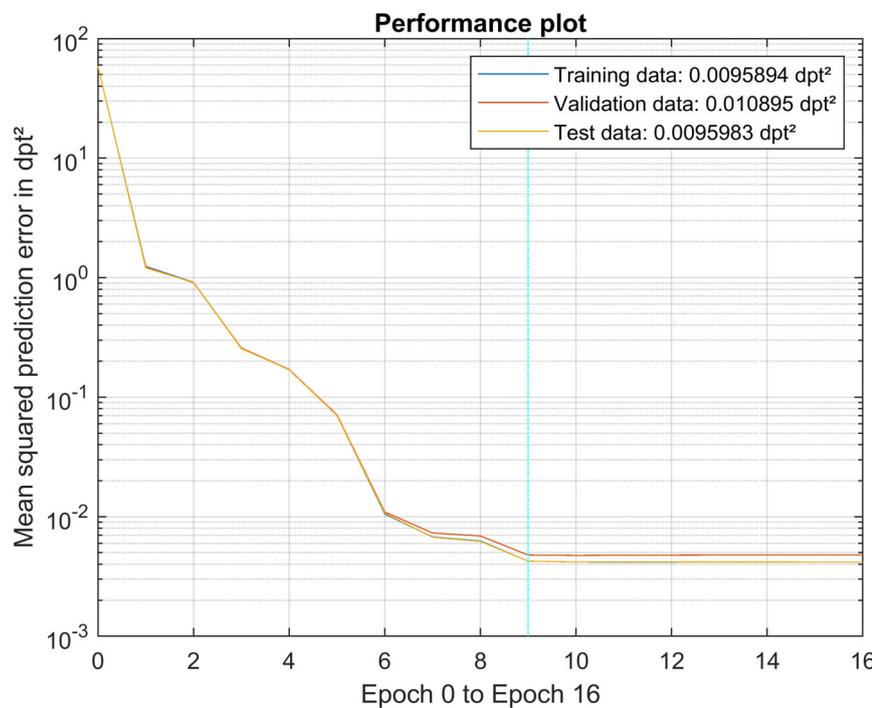
Fig. 1. Performance plot of the shallow feedforward neural network trained for prediction of total corneal power CPpred from the keratometric power K and several biometric measures. After 9 iteration cycles, the final performance was reached as indicated by the cyan line. The respective mean squared prediction error is shown in the legend of the graph.

Table 2. Deviation of the predicted total corneal power CPpred from the total corneal power provided by the IOLMaster 700 biometer (left side) and the deviation of the keratometry measure K from the total corneal power TK (right side) derived from the test dataset in terms of a cross-validation. (.EQ), (.AST0°), and (.AST45°) refer to the equivalent power and astigmatism projected to the 0°/90° and the 45°/135° axis. With the feedforward network the prediction of corneal power based on keratometry and some biometric parameters (age, axial length, central corneal thickness, anterior chamber depth, lens thickness, and horizontal corneal diameter) is much better compared to the keratometry as a measure of corneal front surface data, especially for the astigmatism projected to the 0°/90° meridian

Mean squared prediction error Test data (N = 3166)	CP$_{pred}$-TK in dpt²			K-TK in dpt²		
	CPEQ-TREQ	CPAST$_{0°}$-TRAST$_{0°}$	CPAST$_{45°}$-TRAST$_{45°}$	KEQ-TREQ	KAST$_{0°}$-TRAST$_{0°}$	KAST$_{45°}$-TRAST$_{45°}$
Mean	0.0014	0.0012	−0.0033	0.0028	0.2031	0.0147
Standard deviation	0.0701	0.0686	0.0540	0.1121	0.1071	0.0824
Median	0.0005	0.0012	−0.0048	−0.0011	0.2007	0.0127
Minimum	−0.6567	−0.3531	−0.2680	−0.9152	−0.4202	−0.5037
Maximum	0.6192	0.3311	0.3625	1.0078	0.7297	0.6232
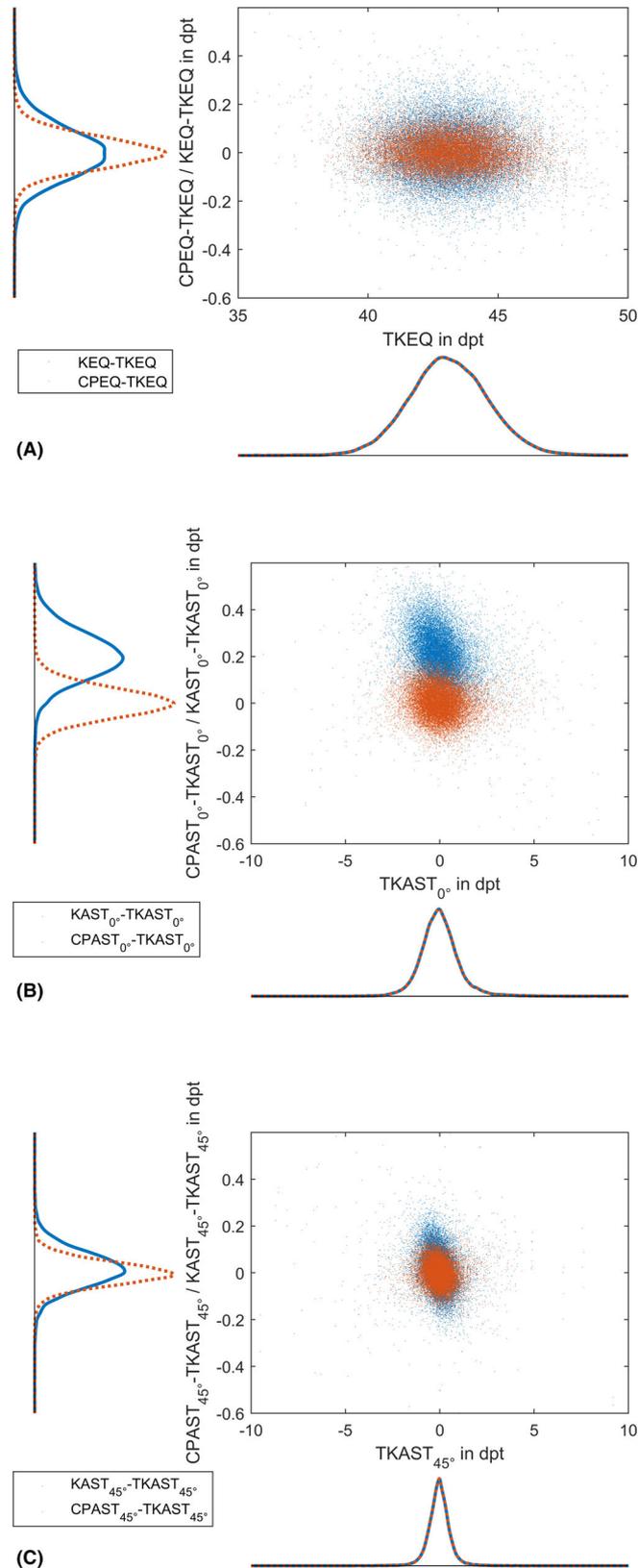
Fig. 2. Combined scatterplot and distribution plot (fitted with a kernel distribution) for the prediction error (predicted corneal power CPpred-total corneal power TK provided by the IOLMaster 700) of the feedforward shallow neural network trained with the $N = 14\,776$ training data set and applied to the $N = 3166$ test data set. As an overlay, the difference between keratometry K from the corneal front surface measurement and total corneal power TK is shown. Subfigures A, B and C refer to the three vector components: equivalent power, astigmatism projected to the 0°/90° axis and astigmatism projected to the 45°/135° axis. In all subfigures, the distribution of the prediction error is narrower compared with the distribution of K-TK, which proves that the prediction model has a good performance. For the astigmatic component in Figure 2B, the distribution is systematically shifted to around −0.2 dpt, which means that the corneal back surface which is considered in TK but not in K adds some astigmatism against the rule (with an axis around 90°).

Table 3. Deviation of the predicted total corneal power CP_{pred} from the total corneal power provided by the IOLMaster 700 biometer derived from the test data set in terms of a cross-validation. (.EQ), (.AST$_{0°}$) and (.AST$_{45°}$) refer to the equivalent power and astigmatism projected to the 0°/90° and the 45°/135° axis, respectively. In this smart version of a feedforward network, while not as good as the results from the full network shown in Table 2, the prediction of corneal power based on keratometry and a reduced number of biometric parameters (axial length, anterior chamber depth and horizontal corneal diameter) is still slightly better in terms of standard deviation compared with the keratometry as a measure of corneal front surface data (especially for the astigmatism projected to the 0°/90° meridian)

Prediction error Simplified neural network Test data ($N = 3166$)	CP_{pred}-TK in dpt		
	CPEQ-TKEQ	CPAST$_{0°}$-TKAST$_{0°}$	CPAST$_{45°}$-TKAST$_{45°}$
Mean	0.0017	0.0005	−0.0005
Standard deviation	0.09383	0.0957	0.09313
Median	−0.0016	0.0013	−.0027
Mean absolute	0.0594	0.0843	0.0454
Minimum	−0.6813	−0.6105	−0.2845
Maximum	0.6737	0.6446	0.4625

provided in Table 2. For the equivalent power/astigmatism component in 0°/90°, and astigmatism component in 45°/135°, the standard deviation is systematically larger, with 0.0938 dpt/0.0957 dpt/0.0931 dpt compared with the full version of the neural network with 0.0701 dpt/0.0686 dpt/0.0540 dpt.

Discussion

It is well known from the literature that, especially for calculation of toric lenses, the total astigmatism of the cornea including the axis cannot be predicted properly by a keratometer (Jaffe & Clayman 1975; Elliott et al. 1994). For eyes with keratometric astigmatism with-the-rule, total corneal astigmatism is decreased, for eyes with keratometric astigmatism, against-the-rule total corneal astigmatism is increased, and with oblique keratometric astigmatism, the axis of the keratometric astigmatism does not coincide with the axis of the total corneal astigmatism. As a consequence, in cases with with-the-rule keratometric astigmatism the cylinder power of toric lenses is normally decreased, and in cases with against-the-rule astigmatism, the cylinder power of toric lenses is increased. In the last decade, several statistical correction strategies or nomograms (LaHood et al. 2017, 2018) have been proposed which estimate the total corneal astigmatism from the keratometric astigmatism (Goggin 2013; Hoffmann et al. 2014; Abulafia et al. 2016; Goggin et al. 2016; Mohammadi et al. 2019; Langenbucher et al. 2021). Most of these strategies are based on a regression analysis (Abulafia et al. 2016; Savini et al. 2017) and an

evaluation of keratometric astigmatism before cataract surgery as well as refraction after cataract surgery with implantation of rotationally symmetric lenses. For example, the Abulafia-Koch regression is derived from spectacle refraction converted from the spectacle plane to the corneal plane and keratometry. Both keratometry and postoperative refraction at corneal plane were transformed to vector components (to the 0°/90° and the 45°/135° meridians; Alpins 1994; Alpins et al. 2004), and the difference of refractive cylinder and corneal astigmatism was quoted as corneal back surface astigmatism. Most of these correction algorithms for the corneal back surface astigmatism add some astigmatic vector in a range 0.1 to 0.3 dpt with an axis against-the-rule (90°) to the cornea (Abulafia et al. 2016; Langenbucher et al. 2021). In some of these correction strategies, the correction depends on the absolute value and/or orientation of the corneal astigmatism before cataract surgery (LaHood et al. 2017, 2018). To overcome a subdivision into with-the-rule, against-the-rule, or oblique astigmatism, and to eliminate potential annealing effects (mostly in the vector component 45°/135°) when mixing left and right eyes, we decided to set up a multi-output neural network which predicts the three output parameters (CPEQ, CPAST$_{0°}$ and CPAST$_{45°}$) in one step from the input parameters KEQ, KAST$_{0°}$ KAST$_{45°}$, AL, CCT, ACD, LT, W2W and the patient's age. Overall, this correction is an estimate from a statistical evaluation of a set of clinical data, and in the individual case, it could be appropriate or result in an over- or under-correction of the real corneal

back surface astigmatism (Reitblat et al. 2016; Savini et al. 2017; Olsen & Jeppesen 2018; Mohammedi et al. 2019; Tutchenko et al. 2020; Nakano et al. 2021).

With the IOLMaster 700, we have the option to measure both corneal surfaces using keratometry and OCT tomography, and with the newer software version, in addition to corneal front and back surface curvature, we can directly read out the composite value TK, which refers to the total keratometry (LaHood et al. 2018; Fisus, Hirnschall & Findl 2021; Fisus, Hirnschall et al. 2021). This total keratometry value is most likely composed from the corneal front and back surface data in addition to the central corneal thickness using some upgraded version of the Gullstrand formula for spherocylindrical surfaces. The first studies on the total keratometry value provided by the IOLMaster 700 show that these data seem to be a good indicator for calculation of toric intraocular lenses (Levron et al. 2021), but further studies with a larger study population have to proof the potential of total keratometry especially for toric lens power calculations.

What we have tried to do in the present study is to predict the total keratometry value TK which is derived from the IOLMaster 700 from keratometric measurement of the cornea (also provided with a classical integrated keratometer) and several biometric parameters such as axial length, central corneal thickness, anterior chamber depth, central thickness of the crystalline lens, plus the horizontal corneal diameter. This means that we did not consider any refraction after cataract surgery, which might be biased on the proper centration and alignment of the intraocular lens as well as the refraction technique and lane distance. Instead of refractometry, we used the measurement of both corneal surfaces on axis with a single measurement. From a large data set which was obtained at two clinical centres and exported using a custom tool, we extracted all preop cataract cases where all relevant measurement parameters including TK were available and where all measurement showed a 'Successful' quality marker in the data output. The keratometric (K) and the total keratometry (TK) measures were algebraically transformed into vector components (equivalent power and projections of astigmatism to the 0°/90° and to the 45°/135° axis) according to the Alpins method (Alpins 1994; Alpins &

Goggin 2004). The keratometric components and the biometric measures were used as input parameters of a shallow multi-output feedforward neural network, and TK was used as the target. In total, $N = 21\,108$ eye measurements were considered, and the data set was split randomly into a training set (70%), a validation set (15%) and a test set (15%) for cross-validation to check for overfitting. In a trial and error sequence, we set up several networks with 2–4 hidden layers and different options for the number of neurons in each hidden layer, together with several training functions. Finally, the Levenberg–Marquardt training function performed best in terms of training speed, number of epochs/iterations and overall performance. In contrast, the quasi-Newton training function did not converge in all cases.

Our results show that the prediction error has distributions for CP_{pred}-TK (CPEQ-TKEQ, $CPAST_{0°}$-$TKAST_{0°}$ and $CPAST_{45°}$-$TKAST_{45°}$) which are much narrower compared with the respective distributions of K-TK. This means that the neural network-based prediction of total corneal power CP_{pred} is in our case better than a prediction, for example, with a constant offset only which is added to the components of K to consider for the astigmatic effect of corneal back surface (Nakano et al. 2021). In addition, we demonstrated that the systematic shift observed in the $KAST_{0°}$-$TKAST_{0°}$ of around -0.2 dpt, which is in accordance with the results of all other correction strategies (e.g. the Goggin correction as shown in Goggin et al. 2015 and Goggin et al. 2016), could be addressed appropriately with our neural network. In addition, if the network is applied to the test data the performance results as shown in Table 2 are not systematically worse compared with applying the network to the entire data set. This means that we do not have a systematic overfitting in our network.

In addition, we tried a smart version of our feedforward neural network by restricting the inputs to those data which are most commonly available during pre-cataract lens power calculation with any optical biometer. To our knowledge, all optical biometers starting from the initial IOLMaster launched in 1999 provide axial length, anterior chamber depth and the horizontal corneal diameter. Together with the patient age and keratometry, the smart neural network was trained with the same training data. As a

result, the performance is somehow worse compared with the neural network considering all biometric measures as outlined above. But in general, the distributions of the prediction error for all three output components are slightly narrower compared with K-TK, and the offset especially in $KAST_{0°}$-$TKAST_0$ could be compensated properly. This means that the performance should be better compared with a static correction of vector components. However, we have to be aware that the precision of the W2W measurement has improved significantly from the first to the latest generation of optical biometers.

In conclusion, this paper shows that with deep learning techniques, the total corneal power as provided in the newest version of the IOLMaster 700 with the TK module could be properly predicted from simple keratometry K, patient age, axial length, anterior chamber depth and the horizontal corneal diameter, and even better if additional data available since the 2nd generation optical biometers such as central corneal thickness or lens thickness are included. In contrast to

a simple vector offset which could easily correct for the static offset of TK-K but does not change the variance of the distribution, the corneal total power prediction CP_{pred} using a feedforward shallow neural network could narrow the distributions of all components of the prediction error CP_{pred}-TK (equivalent power and astigmatic vectors projected to $0°/90°$ and $45°/135°$) and it could correct for the offset.

Authors' contributions

AL involved in conceptualization; investigation; methodology; software; visualization; and writing – original draft. AC involved in formal analysis and validation. NS involved in data curation; formal analysis; project administration; supervision; and validation. JoW involved in formal analysis; conceptualization; and data curation. JaW involved in visualization; conceptualization; and methodology. PH involved in project administration; data acquisition; supervision; and validation.

Glossary

Parameter	Component [unit]	Description
TK	TR1 [mm][A]	Radius of curvature of total keratometry, flat meridian
	TA1 [°][A]	Axis of the flat meridian of total keratometry
	TR2 [mm][A]	Radius of curvature of total keratometry, steep meridian
	TA2 [°][A]	Axis of the steep meridian of total keratometry
	TK1 [dpt][B]	TR1 converted to dioptric power using a keratometer index of 1.332
	TK2 [dpt][B]	TR2 converted to dioptric power using a keratometer index of 1.332
	TKAST [dpt][B]	Total keratometry astigmatism TK2-TK1
	TKEQ [dpt][B]	Equivalent power of total keratometry
	$TKAST_{0°}$ [dpt][B]	Astigmatism vector component at $0°/90°$ of total keratometry
	$TKAST_{45°}$ [dpt][B]	Astigmatism vector component at $45°/135°$ of total keratometry
CP_{pred}	CPEQ [dpt][B]	Equivalent power of the cornea predicted by the neural network
	$CPAST_{0°}$ [dpt][B]	Astigmatism vector component at $0°/90°$ predicted by the neural network
	$CPAST_{45°}$ [dpt][B]	Astigmatism vector component at $45°/135°$ predicted by the neural network
K	R1 [mm][A]	Radius of curvature of corneal front surface, flat meridian
	A1 [°][A]	Axis of the flat meridian of corneal front surface
	R2 [mm][A]	Radius of curvature of corneal front surface, steep meridian
	A2 [°][A]	Axis of the steep meridian of corneal front surface
	K1 [dpt][B]	R1 converted to dioptric power using a keratometer index of 1.332
	K2 [dpt][B]	R2 converted to dioptric power using a keratometer index of 1.332
	KAST [dpt][B]	Keratometric astigmatism K2-K1
	KEQ [dpt][B]	Keratometric equivalent power based on front surface curvature
	$KAST_{0°}$ [dpt][B]	Keratometric astigmatism vector component at $0°/90°$ based on front surface curvature
	$KAST_{45°}$ [dpt][B]	Keratometric astigmatism vector component at $45°/135°$ based on front surface curvature)
AL	[mm][A]	Axial length of the eye
CCT	[mm][A]	Central corneal thickness
ACD	[mm][A]	Phakic anterior chamber depth
LT	[mm][A]	Thickness of the crystalline lens
W2W	[mm][A]	Horizontal diameter of the cornea

Glossary with a description of the abbreviations.
[A]Data directly used from the export file of the IOLMaster 700.
[B]Data calculated as described in the Methods section.

References

Abulafia A, Koch DD, Wang L, Hill WE, Assia EI, Franchina M & Barrett GD (2016): New regression formula for toric intraocular lens calculations. J Cataract Refract Surg **42**: 663–671.

Alpins N (1994): Surgically induced astigmatism. Aust N Z J Ophthalmol **22**: 217.

Alpins NA & Goggin M (2004): Practical astigmatism analysis for refractive outcomes in cataract and refractive surgery. Survey Ophthalmol **49**: 109–122

Chen YA, Hirnschall N & Findl O (2011): Evaluation of 2 new optical biometry devices and comparison with the current gold standard biometer. J Cataract Refract Surg **37**: 513–517.

Elliott M, Callender MG & Elliott DB (1994): Accuracy of Javal's rule in the determination of spectacle astigmatism. Optom vis Sci **71**: 23–26.

Fisus AD, Hirnschall ND & Findl O (2021): Comparison of two swept-source optical coherence tomography-based biometry devices. J Cataract Refract Surg **47**: 87–92. https://doi.org/10.1097/j.jcrs.0000000000000373

Fisus AD, Hirnschall ND, Ruiss M, Pilwachs C, Georgiev S & Findl O (2021): Repeatability of two swept-source optical coherence tomography biometers and one optical low coherence reflectometry biometer. J Cataract Refract Surg **47**: 1302–1307. https://doi.org/10.1097/j.jcrs.0000000000000633

Goggin M (2013): Vector analysis terminology. J Cataract Refract Surg **39**: 1626–1627. https://doi.org10.1016/j.jcrs.2013.08.007

Goggin M, van Zyl L, Caputo S & Esterman A (2016): Outcome of adjustment for posterior corneal curvature in toric intraocular lens calculation and selection. J Cataract Refract Surg **42**: 1441–1448.

Goggin M, Zamora-Alejo K, Esterman A & van Zyl L (2015): Adjustment of anterior corneal astigmatism values to incorporate the likely effect of posterior corneal curvature for toric intraocular lens calculation. J Refract Surg **31**: 98–102.

Haigis W, Lege B, Miller N & Schneider B (2000): Comparison of immersion ultrasound biometry and partial coherence interferometry for intraocular lens calculation according to Haigis. Graefes Arch Clin Exp Ophthalmol **238**: 765–773.

Hoffmann PC, Abraham M, Hirnschall N & Findl O (2014): Prediction of residual astigmatism after cataract surgery using swept source fourier domain optical coherence tomography. Curr Eye Res **39**: 1178–1186.

Jaffe NS & Clayman HM (1975): The pathophysiology of corneal astigmatism after cataract extraction. Trans Am Acad Ophthalmol Otolaryngol **79**:OP615–OP630.

LaHood BR, Goggin M, Beheregaray S, Andrew NH & Esterman A (2018): Comparing total keratometry measurement on the iolmaster 700 with goggin nomogram adjusted anterior keratometry. J Refract Surg **34**: 521–526.

LaHood BR, Goggin M & Esterman A (2017): Assessing the likely effect of posterior corneal curvature on toric IOL calculation for IOLs of 2.50 D or greater cylinder power. J Refract Surg **33**: 730–734.

Langenbucher A, Eppig T, Schröder S, Cayless A & Szentmáry N (2021): Corneal back surface power - interpreting keratometer readings and what predictions can tell us. Z Med Phys **31**: 89–93.

Levron A, El Chehab H, Agard E, Chudzinski R, Billant J & Dot C (2021): Impact of measured total keratometry versus anterior keratometry on the refractive outcomes of the AT TORBI 709-MP toric intraocular lens. Graefes Arch Clin Exp Ophthalmol **259**: 1199–1207.

Mohammadi SF, Khorrami-Nejad M & Hamidirad M (2019): Posterior corneal astigmatism: a review article. Clin Optom (Auckl) **12**: 85–96.

Nakano S, Iida M, Hasegawa Y, Hiraoka T & Oshika T (2021): Influence of posterior corneal astigmatism on the outcomes of toric intraocular lens implantation in eyes with oblique astigmatism. Jpn J Ophthalmol **65**: 288–294.

Olsen T & Jeppesen P (2018): Ray-tracing analysis of the corneal power from Scheimpflug data. J Refract Surg **34**: 45–50.

Reitblat O, Levy A, Kleinmann G, Abulafia A & Assia EI (2016): Effect of posterior corneal astigmatism on power calculation and alignment of toric intraocular lenses: comparison of methodologies. J Cataract Refract Surg **42**: 217–225.

Savini G, Næser K, Schiano-Lomoriello D & Ducoli P (2017): Optimized keratometry and total corneal astigmatism for toric intraocular lens calculation. J Cataract Refract Surg **43**: 1140–1148.

Schmidhuber J (2015): Deep learning in neural networks: an overview. Neural Networks **61**: 85–117.

Tutchenko L, Patel S, Voytsekhivskyy O, Skovron M & Horak O (2020): The impact of changes in corneal back surface astigmatism on the residual astigmatic refractive error following routine uncomplicated phacoemulsification. J Ophthalmol **22**: 7395081.

Zell A (1994): Simulation Neuronaler Netze [Simulation of Neural Networks], 1st edn. Addison-Wesley, p. 73. ISBN 3-89319-554-8.

Correspondence:
Achim Langenbucher
Department of Experimental Ophthalmology
Saarland University
Kirrberger Str 100 Bldg. 22
66424 Homburg
Germany
Tel: +49 6841 1621218
Fax: +49 6841 1621240
Email: achim.langenbucher@uks.eu